Journal of Applied Polymer Science

FEATURE ARTICLE

Novel HDPE/Ground Tyre Rubber Composite Materials Obtained Through *In-Situ* Polymerization and Polymerization Filling Technique

Roberta Sulcis,[1*] Luca Lotti,[1†] Serena Coiai,[2] Francesco Ciardelli,[2,3] Elisa Passaglia[2]

[1]Department of Chemistry and Industrial Chemistry, University of Pisa, Via Risorgimento 35, 56126 Pisa, Italy

[2]CNR-ICCOM UOS Pisa, Via Moruzzi 1, 56124 Pisa, Italy

[3]SPIN-PET s.r.l, Via Risorgimento 35, 56126 Pisa, Italy

*Present address: Fondazione Istituto Italiano di Tecnologia, Via Morego 30, 16163 Genova, Italy

†Present address: Dow Italia s.r.l., Formulated Systems R&D, Via Carpi 29, 42015 Correggio (RE), Italy

Correspondence to: E. Passaglia (E-mail: passaglia@pi.iccom.cnr.it)

ABSTRACT: Novel hybrid materials composed by a high density polyethylene (HDPE) matrix and powdered rubber coming from scrap tyres (*ground tyre rubber* [GTR]) were prepared. Two methods were followed: ethylene was polymerized by a metallocene catalyst (Cp_2ZrCl_2/methylaluminoxane) in the presence of a toluene dispersion of the filler (*in-situ polymerization*); and the ethylene was polymerized out after supporting the aluminum-based co-catalyst onto the rubber particles surface (*polymerization filling technique*). The experimental conditions were varied in order to achieve the best catalyst productivity. All the synthesized composites were characterized in order to investigate the occurrence and the extent of interactions between HDPE macromolecular chains and the GTR components and their effects onto the final properties, by comparison with a composite where GTR was included into the matrix through blending in the melt. Scanning electron microscopy, atomic force microscopy, and solvent extractions were performed to this aim. The amount of thermoplastic matrix bonded to the filler was determined, and the extracted polymer was characterized by size exclusion chromatography and differential scanning calorimetry. Finally, stress–strain behavior of the composites obtained, respectively, by catalytic polymerization and melt mixing was compared. © 2014 Wiley Periodicals, Inc. J. Appl. Polym. Sci. **2014**, *131*, 40313.

KEYWORDS: polyolefins; catalysts; composites; rubber

Received 20 October 2013; accepted 13 December 2013

DOI: 10.1002/app.40313

INTRODUCTION

The disposal of waste polymer rubbers is today a global problem as these materials do not decompose easily;[1] in particular used tyres and their derivatives like *ground tyre rubber* (GTR) are characterized by high chemical stability resulting from crosslinked polymer structure and presence of stabilizers and other additives. Two major approaches to solve this problem are the recycle/reuse of scrap tyres, and the reclaim of the raw materials constituting them. Material manufacturers often include small pieces of scrap tyres in hybrid rubber or thermoplastic/rubber composites; these pieces are granulates (with average particle size lying in the range of 0.5–15 mm) or powders having a particle size inferior to 0.5 mm. The final products obtained from these materials include outdoor sport surfaces, interior floor covering, playground facilities, footwear, inks and paintings, noise absorbing sheets, floor tiles, and paving blocks. Since the economic relevance of these applications is still limited, life cycle thinking is not predominant among tyre producers. This amplifies the importance of research in recycling processes.[2]

The utilization of ground waste rubber in polymer composites has been investigated and reviewed in many studies.[3–10] The GTR has been employed as filler both with rubber and thermoplastic polymers,[11–16] and recently an exhaustive review on this matter has been published by Karger-Kocsis.[17]

The use of pristine/untreated GTR as filler in polyethylene (PE) matrices has not been successful due to surface energy mismatch owing to the nature of components and crosslinked structure of the GTR, leading to incompatibility: surface modification of GTR[18–20] or a suitable compatibilization strategy[21,22] are mandatory in order to improve toughness and possible further properties depending on the matrix. The surface modification is accompanied by increased costs, impairing the production of low-cost GTR-containing composites. Instead, the

Additional Supporting Information may be found in the online version of this article.

use of compatibilizing agents into formulations has been in depth studied and also adopted by some industrial companies which patented compositions/processes aimed at the inclusion of GTR in thermoplastic matrices.[23,24] The most relevant results (discussed in Ref. 17) show the achievement of mature technologies and, in some cases, acceptable final mechanical properties even if both the cost of the most performing compatibilizers and the need of using reinforcing agents make the studied systems complex, and not always commercializable. It is clear that the key role in the obtainment of composites with improved ultimate properties is exerted by the interface interactions, not always enhanced in the reactive compatibilization approaches.

Accordingly, the aim of this article is the preparation and the characterization of GTR/high density polyethylene (HDPE) composites by inclusion of GTR in the thermoplastic matrix through innovative methods based onto the ethylene catalytic polymerization in presence of the substrate. Two methodologies have been used: simple *in-situ polymerization* that means to carry out the polymerization in the presence of swollen GTR particles, and the *polymerization filling technique* (PFT) where the catalyst is interacting with the filler surface.

This latter methodology is widely developed for producing polyolefin-based composites, and it is an efficient way to homogeneously disperse fillers in a polymer matrix up to 95% by volume of inorganics.[25,26] This technique is based on the interactions/reactions of the catalytic system with some functional groups, for instance —OH groups, located on the surface and possibly inside the pores of the filler particles. The polymer chains grow directly from the filler surface or inside the filler pores, and the formed macromolecules cause separation of the filler particles from one another, or could even cause partial disintegration of the latter.

This methodology, if compared with conventional mechanical melt blending, leads to a much more uniform filler distribution and a considerably enhanced interfacial adhesion, even at high filler content.[25] This is a result of the extended desegregation of the filler particles and of their coating by the polymer, and generates, at the same time, an improvement of the mechanical properties of the composite.

The creation of a system active to olefin polymerization is similar for the traditional supported metallocene catalysis (for instance with $MgCl_2$ or SiO_2 as supports) and for PFT. However, in the case of supported catalysis, the support constitutes only the 2–3 wt % of the obtained thermoplastic material, while the amount of filler/support can reach very high amounts (70–80 wt % of the final product) when PFT is adopted. In this latter case, fillers with different nature have been employed in many studies, such as acidic ones (kaolin, other silicates),[26] basic ones [$Mg(OH)_2$, Wollastonite],[26,27] graphite,[28,29] cellulose,[30] and, recently, carbon nanotubes.[31,32] In particular, fillosilicates are the most studied fillers for the preparation of nanocomposites having a HDPE-matrix by means of PFT.[33–36] The most adopted catalysts for olefin polymerization are: the *Constrained Geometry Catalyst* (*CGC*; [$(Cp^*)SiMe_2(N\text{-}tertBu)$]-$TiCl_2$),[33] zirconocene dichloride (Cp_2ZrCl_2),[37] other ansa-metallocenic compounds,[36] and also Ziegler–Natta catalysts.[35] Mülhaupt et al. also adopted water-soluble Ni- and Pd-based catalysts for olefin polymerization.[38] The complex chemical composition of the fillers significantly affects the catalytic properties, which vary from substrate to substrate. The catalytic activity in PFT systems is often lower than in supported systems, and there is a study on the kinetics of PFT that points out this difference.[39]

In the present study, the exploitation of the PFT in comparison with the *polymerization in situ* methodology was targeted as a tool to prepare thermoplastic–elastomeric materials by using GTR, in order to realize a better phase dispersion with respect to the simple mixing of the components and the creation of interactions located at the interface deriving from functional groups of the two phases or from the formation of a semi-interpenetrating polymer network (sIPN).

Analogously to what is reported in prior art for silicates, the authors of the present study applied the PFT by treating the filler (GTR in this study) with the co-catalyst and the metallocene (or *vice-versa*) prior to the ethylene introduction in the system. In order to favor the establishment of interactions between the PE growing chains and GTR during the polymerization process, a catalyst system (Cp_2ZrCl_2 activated by MAO) working in a solvent (toluene) able to swell rubber particles was selected. The *in-situ* polymerization process was performed and compared with the PFT method by polymerizing the ethylene in the presence of swollen GTR, but without supporting the catalyst.

EXPERIMENTAL

Materials

Monomers: Ethylene (Rivoira S.p.A., polymerization grade 99.9%) was used as received. *Polymers*: PE homopolymer [Total, HDPE Lacqtene(TM) 2070 M 60], with a melt flow rate (MFR) of 20.0 g/10 min (200°C/5 kg, ISO 1133), density of 969 kg/m^3 (ISO 1183), elongation at break >700% (ISO 527-2), and melting temperature (T_m) of 135°C (ISO 3146) according to the supplier data sheet, was used without any purification process. *Filler*: GTR particles collected by tyres recycling and kindly supplied by Pirelli Labs S.p.A., were used. The powder was extracted with both boiling acetone and toluene before the use (Kumagawa extractor, 16 hours) in order to remove extending oils, vulcanization additives and stabilizers, and finally dried under vacuum until constant weight. A detailed characterization is reported in a previous publication.[40] *Catalyst and solvents:* *bis*(cyclopentadienyl)zirconium(IV) dichloride (zirconocene dichloride, Cp_2ZrCl_2, Aldrich, 95%) and methylaluminoxane (MAO, $(Al(CH_3)O)_n$, Crompton, 10 wt % in toluene) were used without any further purification. Toluene (Baker, 99.8+%) was distilled over Na/K alloy and stored under argon. Methanol (Baker, 99.5%), xylene (isomers plus ethylbenzene, Aldrich, 98.5%), acetone (Carlo Erba, RP grade 99.9+%), and hydrochloric acid (Baker, 37 wt % water solution) were used without any further purification.

Catalytic Homopolymerization of Ethylene in the Presence of GTR

All the described operations were performed in moistureless and oxygen-free conditions, with the use of an argon-vacuum

system and standard schlenk techniques. All the polymerizations were performed in a 200 mL glass reactor vessel (Büchi) equipped with a mechanical stirrer.

The average productivity values (average polymerization rate over a period of time of the polymerization process) were determined according to the following eq. (1):

$$\text{Average productivity} = \frac{m_{PE}}{n_{Zr} \times t \times p_{CH_2CH_2}} \quad (1)$$

where m_{PE} is the amount in kilograms of PE formed during the polymerization; n_{Zr} is the molar amount of zirconocene dichloride; t the reaction time (in hours); $p_{CH_2CH_2}$ is the ethylene pressure (in bars) applied during the polymerization process.

The grafting yield (*G.E.*) was calculated by using the eq. (2):

$$G.E. = \frac{m_{\text{unextracted PE}}}{m_{\text{total PE}}} \times 100 \quad (2)$$

where $m_{\text{unextracted PE}}$ is the mass of PE not extractable with boiling xylene (mixture of isomers) in a Kumagawa extractor for 16 hours, and $m_{\text{total PE}}$ is the mass of PE introduced into the extractor.

Polymerization of Ethylene with Zirconocene Dichloride

In a typical experiment, 0.5 g of GTR is swollen overnight in 10 mL of toluene in a 25 mL schlenk tube. In the *in-situ* polymerization method, 10 mL (15 mmol) of MAO solution in toluene, and 1 mL (15 μmol) of a 0.015*M* solution of Cp_2ZrCl_2 in toluene are added in rapid succession to the initial GTR suspension, and kept for 10 min at room temperature (aluminium/zirconium [Al/Zr] molar ratio: 1000).

In the PFT method, first the co-catalyst is supported onto the filler: 10 mL (15 mmol) of MAO solution in toluene is added to the initial GTR suspension; this amount has been varied with respect to the chosen Al/Zr ratio (see the section Results and Discussion). The mixture is magnetically stirred at 60°C for 60 min. Afterward, 1 mL (15 μmol) of a 0.015*M* solution of Cp_2ZrCl_2 in toluene is added and allowed to react with the MAO-treated filler at 80°C for 150 min before being transferred into the reactor.

In both cases, after the generation of catalytic system, the slurry with GTR particles, MAO and the metallocene is transferred into the reaction vessel containing 80 mL of freshly distilled toluene under positive pressure of argon; the reaction mixture is void-degassed, and then a pressure of ethylene is applied. The experiments of the present study were carried out under a constant, 2-bar pressure of ethylene. The polymerization runs, performed at different reaction times (see the section Results and Discussion), are quenched by the addition of 10 mL of a 5 vol % $HCl_{(aq)}$/MeOH solution. The polymeric product is recovered by filtration; it is eventually washed with abundant MeOH and dried under vacuum until constant weight.

Preparation of GTR/HDPE Composites by Melt Mixing

Two mixings of commercial HDPE and GTR particles were prepared in a Brabender Plastograph PL2100 mixer at 180°C; in a first instance (i) pristine GTR was added (sample SimpleMix), while in a second instance (ii) a masterbatch compound (obtained through the PFT technique) containing 73.6 wt % of PE and 26.4 wt % of GTR was added (sample ComplexMix). For both experiments, the rotor speed is initially set at 50 rpm and the instrument is let swelling for calibration under nitrogen flux in the mixing chamber; then the HDPE is added. The mixing chamber is closed with a V-shaped steel closure, and the polymer is melt blended for 1 min; afterward, the GTR or the masterbatch is added. The mixing is carried out for 15 min; then, after 15 min, the rotors are stopped, the chamber opened, and the composite material recovered.

In instance (i) 20.0 g of HDPE and 2.4 g of GTR (added after 1 min) are employed; and in instance (ii) 13.3 g of HDPE and 9.0 g of masterbatch containing 73.6 wt % of PE (added, again, after 1 min) are employed. In both cases, 24.7 g of materials are mixed, and in both cases the amount of GTR in the final composites is 8.8 wt %.

Characterizations

The Fourier transform infrared spectra (FT-IR) were collected at room temperature by a Fourier Transform Spectrometer Perkin Elmer FT-IR 1760-X. The attenuated total reflectance-infrared (ATR-IR) spectra were collected at room temperature by using a Perkin Elmer Spectrum GX instrument equipped with the horizontal attenuated total reflectance tool.

^{1}H-NMR and ^{13}C-NMR spectra were performed by a spectrometer Varian Gemini 200 MHz and with a Varian VXR 300 MHz instrument, respectively. The spectra were collected at 120°C using 1,1,2,2-tetrachloro-1,2-dideuteroethane (TCE-d_2) as solvent; chemical shifts were assigned in parts per million (ppm) using the solvent signal as internal standard.

Differential scanning calorimetry (DSC) analyses were performed by a Perkin Elmer DSC7 calorimeter equipped with a *CCA7* cooling device using 10–15 mg of sample under nitrogen flux. Heating and cooling thermograms were carried out at a standard temperature rate of 20°C/min; the crystallization process of PE matrix in the composites was observed after a first heating of specimens above 170°C.

All TGA thermograms were recorded by a Mettler Toledo Star System TGA/SDTA 851 instrument. Samples of 5–10 mg were placed in alumina pans; runs were carried out at a standard temperature rate of 10°C/min from (i) 25°C to 600°C under nitrogen flow, and (ii) from 600°C to 1100°C under air flow. The *onset* temperature was taken as the temperature of degradation.

Tensile properties were determined with a Tinius-Olsen H10KT High Force Dynamometer. Specimens for tensile testing and measurements were obtained at room temperature according to the ASTM D-638; of ten specimens were provided for each sample, and the average measurement values were reported.

All scanning electron microscopy (SEM) micrographs were performed with a *Jeol 5600-LV* instrument equipped with an Oxford X-ray energy dispersive spectrometer (EDXS) microprobe. The analyzed surface was obtained after gold-metallization of a cryogenic fracture of the composite. By using EDXS, the elemental composition of non-metallized materials was obtained with high spatial resolution by measuring the energy or

Table I. Preliminary Ethylene Polymerizations Carried Out with the Cp_2ZrCl_2/MAO System; Polymerization Time = 1 Hour

Sample	GTR (g)	Conditions	Productivity $kg_{PE}/(n_{Zr}$ bar hour)	GTR in the composite (wt %) [a]	GTR in the composite (wt %) [b]	Grafting yield (wt %) [c]	DSC data T_m (°C)	DSC data ΔH_m (J/g) [d]	DSC data α [e]
PE 1	—	MAO + Cp_2ZrCl_2 (10 min at R.T.)	517 ± 29	—	—	—	136.2	202.5	75
PE 2	—	MAO (60 min at 60°C) + Cp_2ZrCl_2 (150 min at 80°C)	182 ± 10	—	—	—	136.4	191.9	71
PEP 1[f]	0.5	MAO + Cp_2ZrCl_2 (10 min at R.T.)	464 ± 26	3.5	2.3	~0	136.7	191.3	71
PEP 2[g]	0.5	MAO (60 min at 60°C) + Cp_2ZrCl_2 (150 min at 80°C)	177 ± 10	8.8	8.9	11.9	135.7	163.9	61
PEP 3[g]	0.5	Cp_2ZrCl_2 (60 min at 60°C) + MAO (150 min at 80°C)	68 ± 4	19.8	11.8	9.6	132.0	36.6	14

[a] By mass balance.
[b] By TGA experiments.
[c] The *G.E.* is defined as the amount of PE unextractable from the composite (extraction in Kumagawa, 16-hours, refluxing xylene).
[d] Normalized with respect to the PE content (in grams) in the composite.
[e] α = % crystallinity ($\Delta H_{m,sample}$/(269.9 J/g). The value ΔH_m = 269.9 J/g is referred to 100% crystalline PE.
[f] *In-situ* polymerization method.
[g] PFT method.

wavelength and intensity distribution of X-ray signals generated by a focused electron beam. The calibration of EDXS for quantitative determination of elements was done by evaluating the intensity data of a microanalysis certified sample with a known composition (Biological Block standard for EDXS in SEM, MAC Micro Analysis Consultants).

Atomic force microscopy (AFM) micrographs were obtained with a Nanoscope IIIa scanning probe microscope on flat specimens obtained by using an ultramicrotome (Leica Ultracut UCT) equipped with a Leica EM FCS cryochamber. Height and phase images were obtained simultaneously, while operating in tapping mode under ambient conditions. Images were taken using standard micro fabricated silicon cantilevers with an aluminum reflecting coating (Nanoworld, Arrow NC-50). The cantilevers had normal spring constants of 13–70 N/m and typical resonance frequencies between 250 and 315 kHz. Typical scan speeds during recording were 0.3–1.5 line/s using scan heads with a maximum range of 30 × 30 μm. The phase images represent the variation of relative phase shift, that is, the phase angle of the oscillating cantilever relative to the phase angle of the freely oscillating cantilever at the resonance frequency.

Size-exclusion chromatography (SEC) was performed with a Waters Alliance GPCV-2000 Series System apparatus equipped with three Waters Styragel HT 6E columns (MW: 5000–100,00,00 Da) and one Waters Styragel HT 3 [molecular weight (MW): 500–30,000 Da] column; the instrument was also equipped with a differential refractive index (DRI) detector. Polymer solutions for the injection were prepared by dissolving 4 mg of polymer in 8 mL of 1,2,4-trichlorobenzene (TCB) containing a little amount of an antioxidant (butylated hydroxytoluene [BHT], 1 wt %) to prevent any degradation. The samples were eluted at 145°C with a flow rate of 1 mL/min. The SEC calibration was performed by eluting polystyrene standards having narrow molecular weight dispersion (kindly furnished by Sigma-Aldrich Company).

RESULTS AND DISCUSSION

Preliminary Polymerization Experiments

The first part of the study is focused on the tuning of experimental conditions for the metallocene-mediated polymerization of ethylene in the presence of GTR, and on the comparison between PFT and simple *in-situ* polymerization methodologies. The catalytic system adopted is the Cp_2ZrCl_2/MAO catalyst, already investigated in prior art for similar synthesis.[37] Three methodologies were compared: (i) simple *in situ* polymerization without supporting the catalyst, (ii) PFT carried out by supporting the aluminum-based co-catalyst followed by addition of metallocene, and (iii) PFT carried out by supporting the metallocene before MAO activation. The polymerization runs, carried out under a constant pressure of ethylene, in dry toluene and with an initial Al/Zr molar ratio of 1000 (literature values vary, for analogous systems, from 600[27] to 2000[37]), are described and compared with blank runs in Table I in terms of catalyst productivity, amount of filler in the composite, *G.E.* (defined as the percentage of PE unextractable from the composite after solvent extraction), and melting/crystallization behavior.

Comparing the catalyst productivities of PE 1 and PEP 1 experiments (simple *in-situ* polymerizations), a approximately

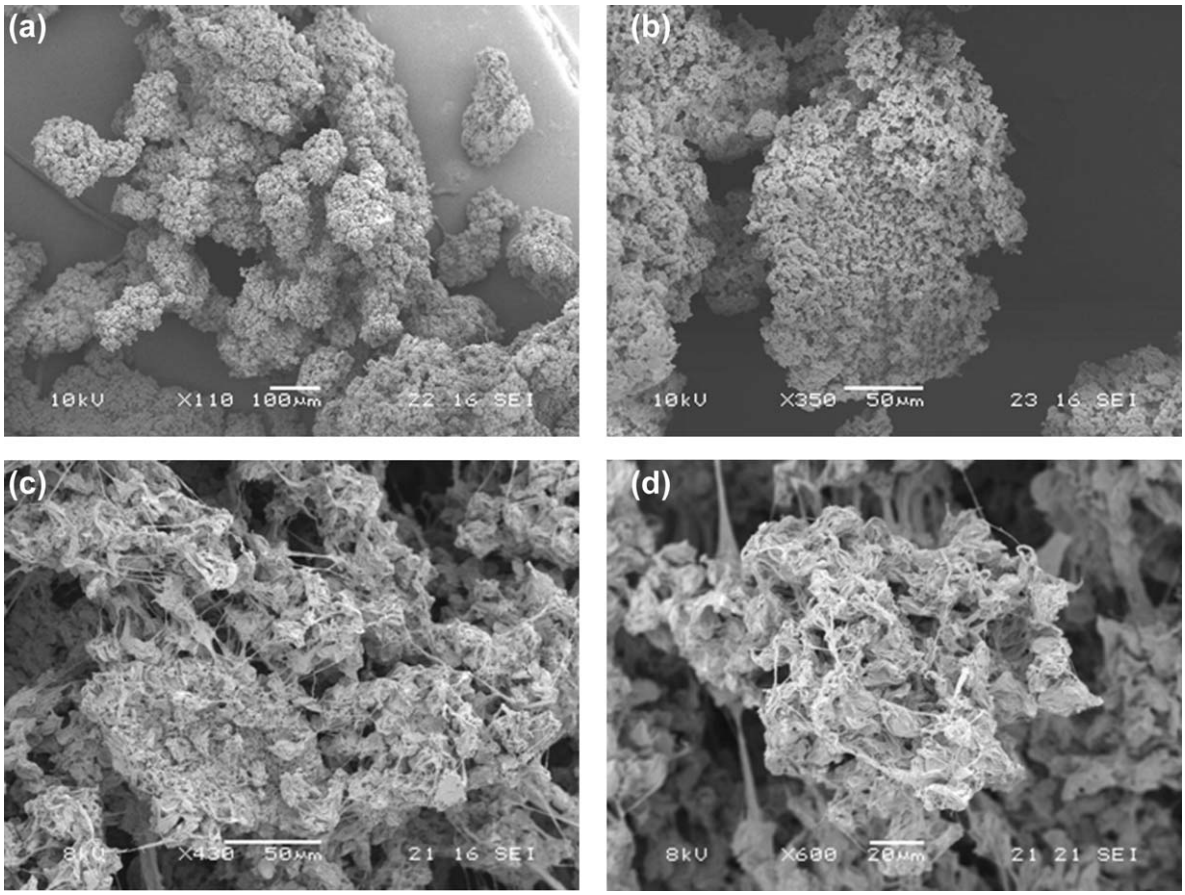

Figure 1. Scanning electron microscope pictures of PEP 2 (**a**,**b**) and PEP 2 after xylene extraction (**c**,**d**).

10% decrement is observed. This is probably due to the hydrolysis reaction of MAO with silanol and carbinol groups which are present on the surface of GTR particles, as demonstrated by IR analysis.[40] The decrement is reduced to about 3% in the PE 2 and the PEP 2 runs (*PFT*-polymerizations): the ageing time of MAO at 60°C for 60 min before the addition of the metallocene and the ageing time of Cp_2ZrCl_2, caused also a significant decrease of productivity value both with and without GTR (PE 1 vs. PE 2; PEP 1 vs. PEP 2): the catalyst productivity was reduced of about 60%–65% in both cases as observed in prior art.[41]

The effect of the reagent addition order on the catalyst productivity was investigated in PEP 3 run. In this case the metallocene complex was first added to the rubber particles swollen in toluene, and allowed to react for 60 min at 60°C; then MAO was added and allowed to react at 80°C for 150 min before starting the polymerization. The catalyst productivity was remarkably reduced, and the obtained composite was very heterogeneous as confirmed by thermogravimetric and morphological analyses. In particular, the amount of included rubber ranged from 11.8 (by TGA) to 19.8 wt % (by mass balance); this remarkable discrepancy between the two values is not new in PFT studies[41] regarding similar systems, and has been attributed to a non-homogeneous distribution of the phases (PE/GTR) in the sample. On the contrary, for the other composites, the difference between the two values is lower (see Table I) and, accordingly, the samples looked more homogeneous. The reduced catalyst productivity of PEP 3 experiment is probably due to partial poisoning of the metallocene complex by some of the components present in the filler itself; if MAO is added before the transition metal complex, instead, the co-catalyst could act as a scavenger of the impurities thus protecting the metallocene and causing only a limited decrease in the activity as hypothesized in many studies regarding PFT or *in situ* polymerisations.[34,37,42,43]

Composites Properties

The thermal properties of the samples were investigated by using DSC measurements; melting temperatures (T_ms) are reported in Table I. The T_m of the PE matrix in the composites was very similar for all the samples and featured the thermal behavior of HDPE pure samples. The associated enthalpy values (ΔH_m) decreased at higher amounts of GTR in the composite; the crystallinity (α), calculated on the PE fraction of the composites, seemed to be affected by the conditioning of GTR particles with MAO, (PEP 1 vs. PEP 2 runs), and thus by the adopted PFT methodology and decreased by increasing the time of ageing of the catalyst onto the particles. PEP 3 sample showed lower values of T_m and α; these data could be related to the method used (PFT) in preparing GTR-supported metallocene catalyst and/or to the relatively high amount of GTR in the composite.

All the composites were washed in a Kumagawa extractor for 16 hours with boiling xylene (a good solvent for PE) in order to

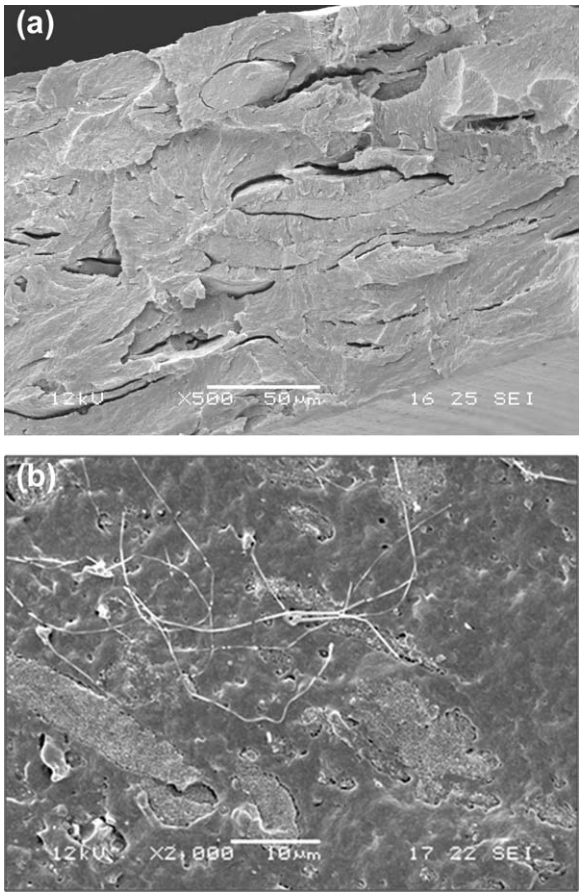

Figure 2. Scanning electron microscope pictures of PEP 1 (**a**) and PEP 2 (**b**) after cryogenic fracture of press-molded specimens.

estimate the amount of PE not extractable from the samples due to strong interactions with the filler. The most interesting result is that PEP 2 and PEP 3 samples showed similar grafting efficiencies (Table I) although they had a different content of PE and were prepared with different methodologies; this experimental evidence indicates that the amount of PE strongly interacting with GTR does not directly depend on the order of addition of MAO or Cp_2ZrCl_2 to the filler suspension, but will rather depend on the long times employed to support the catalyst on GTR.

Spectroscopic measurements (IR, ^{1}H-, and ^{13}C-NMR) did not highlight substantial differences, in terms of primary structure, between PE blank runs (PE 1/PE 2) and PE samples extracted from respective runs carried out in presence of GTR (PEP 1/PEP 2). In particular, the ^{13}C-NMR spectra of all the cited samples showed only a single peak at $\delta = 31.1$ ppm accounting for secondary carbons located in the main chain; tertiary carbons were not detected and, considering the signal/noise ratio of the used instrument, it was possible to roughly evaluate the number of branches, lower than 1 over 12,000 carbon atoms (see Supporting Information).

The images derived from SEM of PEP 2 sample [Figure 1(a,b)] showed that the PE uniformly covered the filler particles, forming globular masses; this could account for the presence of catalytic centers on the surface or even inside the GTR particles.

The images of the residuals after solvent extraction showed that the dimensions of the rubber particles decreased with respect to the starting ones, and were interconnected by a dense network of PE, thus confirming strong interactions at the interface [Figure 1(c,d)].

SEM micrographs of cryogenic fracture surfaces from PEP 1 and PEP 2, reported in Figure 2(a,b), respectively, showed two main evidences: (i) the filler is segregated from the PE matrix in PEP 1 sample (provided by *polymerization in-situ*), and large cracking is observed (no adhesion can be highlighted). This does not occur in PEP 2, which was obtained by PFT; (ii) the shape of filler particles in PEP 2 is irregular and vesicles of PE inside the particles can be identified.

The morphology of composites PEP 1 and PEP 2 at the interface matrix/filler was also investigated by means of AFM. Phase images of PEP 1 [Figure 3(a,b)] show that the interface is well defined even at high magnitudes; on the contrary, by applying the PFT methodology (sample PEP 2) [Figure 3(c,d)] the formation of PE domains in the bulk of filler particles can be evidenced, thus suggesting the occurrence of ethylene polymerization inside the particles. Moreover, the growth of macromolecular chains inside GTR causes the breakup of the particles, and this phenomenon is well visible in the last micrograph of Figure 3(d).

Based on optical microscopy images of PEP 1 and PEP 2, an analysis of the GTR particles distribution in terms of (a) perimeter, (b) diameter, and (c) area was carried out by using the Scanning Probe Imaging Processor (SPIP, ©Image Metrology V 4.3.1.0). This analysis, usually called *Grain Analysis*, is used for the detection and quantification of grains/pores or other regions for which the boundaries can be defined based on the microscope image. In the case presented in this study, this experiment clearly showed that the distributions of the diameter, perimeter, and area of PEP 2 particles were broader than the ones of PEP 1 particles (Table II). This increment suggests, again, the growing of PE macromolecules inside the GTR particles; moreover, the remarkable increase in the length of the interface (i.e., the perimeter) could account for a crumpling effect due to the same phenomenon.

Nature of the MAO–GTR Interaction

The main features of the supported co-catalyst (GTR/MAO intermediate) were studied by IR and SEM/EDXS elemental characterizations to highlight possible reactions/interactions.

It is known that MAO and carbinol/silanol groups can react to form a rather stable X—O—Al bond, where X = Si or C. On this basis, the interactions of both Cp_2Zr^+Me and Cl^- with MAO anchored onto GTR particles can be postulated similarly to the case of a silica support treated with aluminoxane.[44]

In order to characterize newly formed C—O—Al or Si—O—Al bonds, the ATR-IR spectrum of pristine GTR was compared with: (i) the spectrum of a GTR/MAO adduct obtained by mixing the swollen GTR with MAO followed by immediate toluene washings; (ii) the adduct of point (i) treated for 1 hour at 60°C and washed with toluene (in both cases, the non-grafted MAO

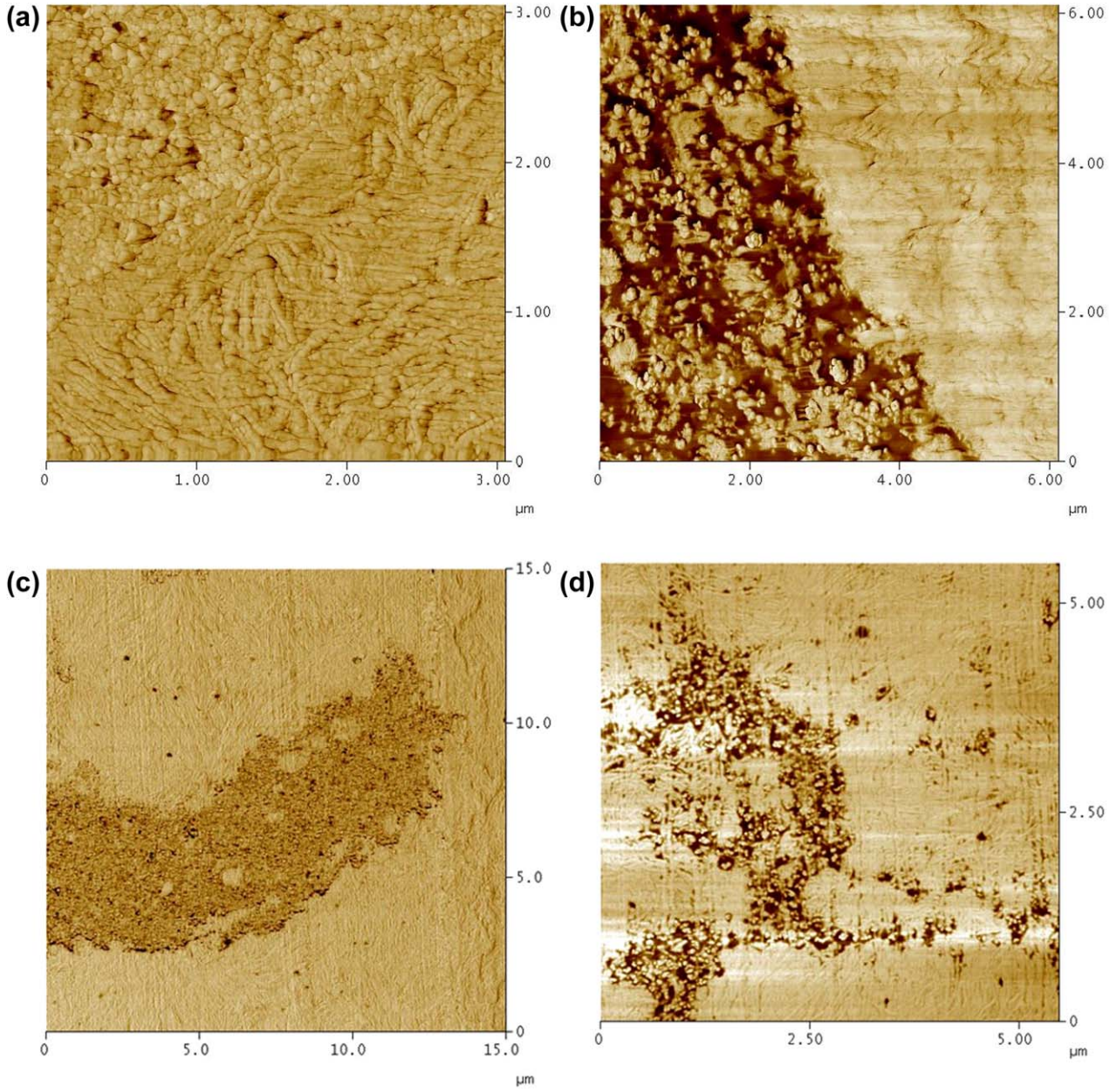

Figure 3. AFM phase images of PEP 1 (**a**,**b**) showing neat PE/GTR interface, and PEP 2 (**c**,**d**) showing, respectively, vesicles of PE inside GTR and GTR disintegration. [Color figure can be viewed in the online issue, which is available at wileyonlinelibrary.com.]

chains are supposed to be washed away). The used amounts are those of the experiments described in Table I.

In the collected spectra, the assignment of IR bands at 900–1100 cm^{-1} was difficult because of the very broad signal of silica (Al—O stretching fall in the 900–950 cm^{-1} range); also the identification of MAO methyl group bending (around 1400 cm^{-1}) was difficult because of GTR bands. On the other side, it was possible to identify the presence of Al-bonded methyl groups in the C—H stretching zone (Figure 4).

The bands of pristine GTR are: 2955 cm^{-1} (ν_{as} CH_3; ν_s CH_3 is hidden, around 2870 cm^{-1}), 2920 cm^{-1} (ν_{as} CH_2) and 2845 cm^{-1} (ν_s CH_2). These two bands undergo a strong

Table II. Dimensional Data (Mean, Minimum, and Maximum) of GTR Particles Dispersed in PEP 1 and PEP 2 Samples

Sample		Diameter (µm)	Perimeter (µm)	Area (µm ^{2})
PEP 1	Mean	34	580	1420
	Minimum	13	199	1230
	Maximum	93	648	6780
PEP 2	Mean	59	493	3720
	Minimum	21	106	3350
	Maximum	145	1570	16300

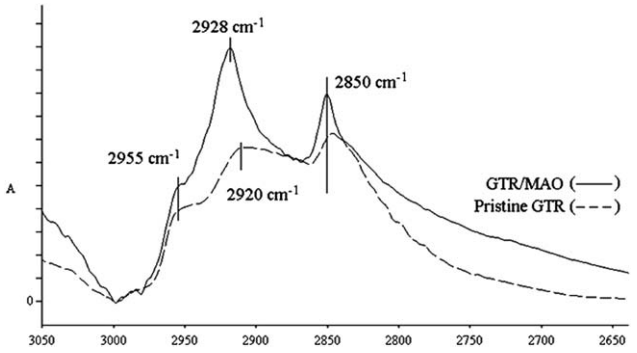

Figure 4. Comparison between ATR spectra (in the range 3050–2650 cm $^{-1}$) of GTR and GTR/MAO adduct.

intensification after MAO introduction, and their maximum peak results quite shifted, of about approximately 25 cm^{-1}, with respect to aliphatic carbon compounds as these —CH_3 groups are presumably bonded to Al atoms.[45] A new band at 2928 cm^{-1} (ν_{as} CH_3) and another one at 2850 cm^{-1} (ν_s CH_3) appear and overlap, respectively, the methylene asymmetric and symmetric stretching due to GTR elastomeric chains.

In order to establish if any interaction between the zirconium complex and supported MAO was possible, as suggested by Chien and He[44], an IR characterization of the GTR/MAO/metallocene system was performed. After supporting MAO (60 min at 60°C) onto GTR, a toluene solution of zirconocene dichloride was added; the system was then treated for 150 min at 80°C and washed several times with toluene at room temperature. The presence of the complex in the product was confirmed by the IR absorption at 3018 cm^{-1} (Figure 5) that may be attributed to the C—H stretching belonging to the cyclopentadienic rings of the metallocene. Usually this band falls at about 3100 cm^{-1} in the dichloride complex; it can be supposed that the particular interaction between the zirconium atom and MAO could have caused a similar shift. This hypothesis was first suggested by Zimnoch dos Santos et al.[46] on the basis of observations performed on (n-BuCp)$_2$$ZrCl_2$ supported onto silica.

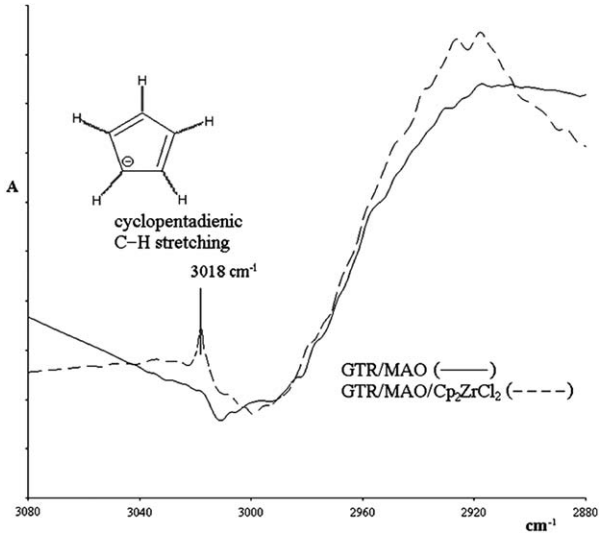

Figure 5. Comparison between ATR spectra (in the range 3080–2880 cm $^{-1}$) of GTR/MAO adduct and GTR/MAO/Cp_2ZrCl_2 supported catalyst.

The mechanism for the MAO anchoring and the interactions between species resulting from Cp_2ZrCl_2 reaction with MAO itself, as suggested by IR spectra, is reported in Scheme 1 with a sketch of possible adducts.

The interaction between GTR and MAO was also evidenced by the formation of a wrinkled coating onto the GTR particles; a similar observation was performed by Dubois et al. in a study concerning the obtainment of PE/carbon nanotubes composites by using a $Cp^*_2ZrCl_2$/MAO catalyst system by treating the filler on the basis of the PFT.[31] A SEM micrograph of GTR particles after MAO addition is reported in Figure 6.

Moreover, the atomic surface composition of GTR particles after supporting the co-catalyst, determined with EDXS analysis, revealed a remarkable increase in the relative percentage of aluminum and oxygen (Al: from 0.23 wt % to 18.61 wt %; O: from 22.81 wt % to 54.27 wt %). After the metallocene

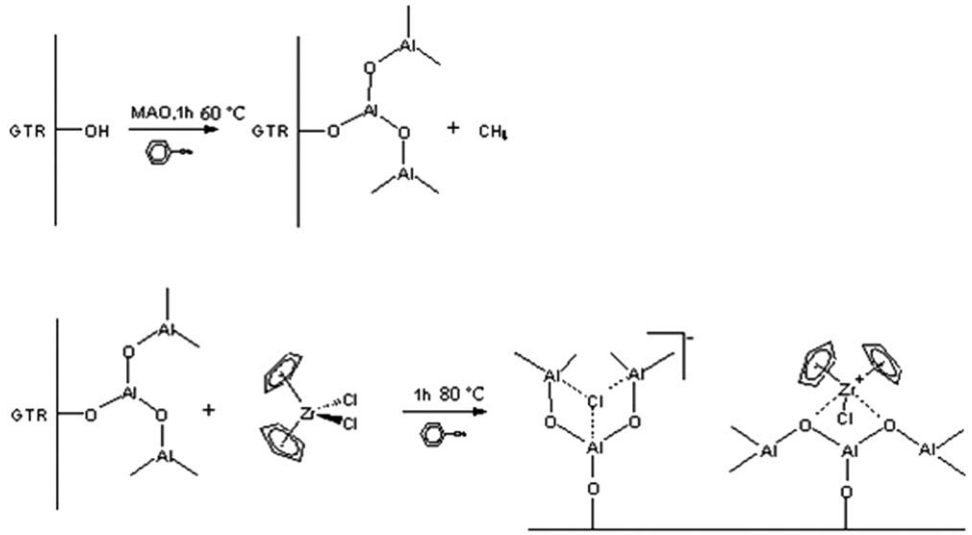

Scheme 1. Possible mechanism providing the GTR-supported catalyst system.

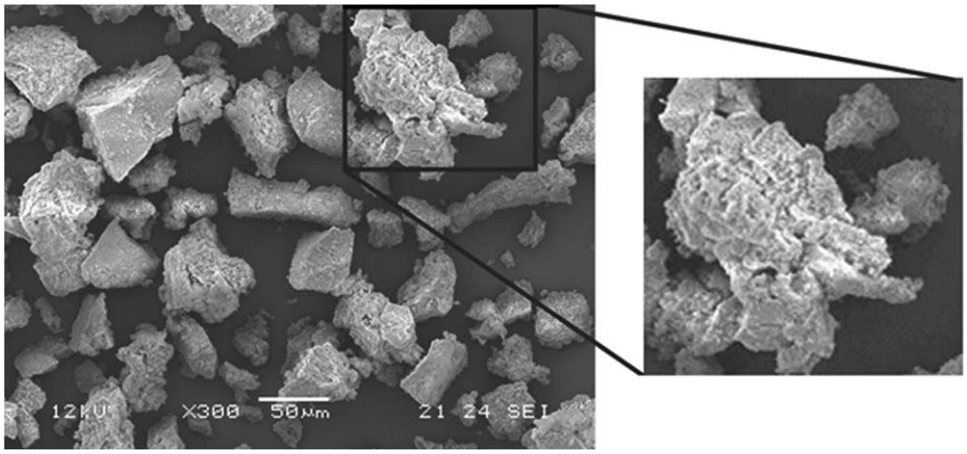

Figure 6. SEM micrograph of GTR particles after MAO reaction.

addition, instead, EDXS did not highlight the Zr presence, and this is probably due to the very low amount of added metallocene, below the detection limit of this technique.

Effect of Co-catalyst/Metallocene Ratio Variation

The effect of the variation of the Al/Zr molar ratio on the properties of the catalyst system and, consequently, on the obtained composite materials was studied by employing different amounts of co-catalyst keeping a constant Cp_2ZrCl_2/GTR ratio (15 μmol/0.5 g). The catalyst productivity of each run, the composition of the corresponding composites and the grafting yields are reported in Table III.

The composition of the samples was determined both by mass balance and by TGA. By increasing the Al/Zr molar ratios, the amount of PE in the composites reached a *plateau* for a value higher than approximately 500 suggesting the achievement of a maximum number of active sites.

DSC scans of the samples in the 40°C–180°C range showed T_m in the range 135°C–137°C without meaningful variations, while the related enthalpies decreased by increasing Al/Zr molar ratio (Table III). To better understand this trend, a study concerning the possible presence of different PE macromolecular chains was carried out; this study included selective solvent extractions and fraction characterizations.

A first separation was carried out, as previously did on preliminary samples, by extracting the PE with boiling xylene. The grafting efficiency, listed in Table III, showed no substantial variations between the samples ranging from 9.0 to 11.9 wt %; on the basis of these data, one can conclude that the Al/Zr molar ratio did not affect significantly the amount of active centers producing not-extractable PE chains.

In Table IV SEC data as well as thermal properties regarding residual and extracted fractions are reported (only the extracted parts of the samples could be analyzed with SEC equipment for the MW determination).

The $<M_w>$ values range between 400 and 600 kDa, in agreement with typical $<M_w>$s of GTR-free polymerizations; for instance, PE 2 (Table I, same Al/Zr ratio of PEP 1000 but carried out in

Table III. Experiments with Different Al/Zr Initial Molar Ratios[a] (Time of Polymerization = 1 Hour)

			GTR in the composite			DSC data		
Sample [b]	Al/Zr molar ratio	Productivity $kg_{PE}/(n_{Zr}$ bar hour)	(wt %)[c]	(wt %)[d]	Grafting yield (wt %) [e]	T_m (°C)	ΔH_m (J/g)[f]	α[g]
PEP 1000	1000	177 ± 10	8.8	8.9	11.9	135.7	163.9	61
PEP 700	700	155 ± 9	9.7	10.9	10.0	136.1	175.4	65
PEP 500	500	110 ± 6	16.6	16.3	11.4	136.6	191.4	71
PEP 300	300	48 ± 3	42.6	40.7	9.0	135.8	213.0	79
PEP 200	200	~0	~100	97.9	—	—	—	—

[a] PE/GTR composites obtained with different Al/Zr ratios were named with the symbol PEP k where k is the Al/Zr molar ratio used in the corresponding polymerization run.
[b] Catalytic system: GTR (toluene suspension) + MAO (60′ at 60°C) + Cp_2ZrCl_2 (150′ at 80°C).
[c] By mass balance.
[d] By TGA experiments.
[e] The *G.E.* is defined as the amount of PE not removable from the composite (extraction in Kumagawa, 16-hours, refluxing xylene).
[f] Normalized with respect to the PE content (in grams) in the composite.
[g] α = % crystallinity = $\Delta H_{m,sample}/(269.9$ J/g). The value $\Delta H_m = 269.9$ J/g is referred to 100% crystalline PE.

Table IV. SEC Measurements and Thermal Properties (by DSC) of the PEP Produced by Changing the Al/Zr Initial Molar Ratios Samples After Xylene Extraction

Sample [a]		$<M_n>$ ($<M_w>$) kDa	MWD	DSC data		
				T_m (°C)	ΔH_m (J/g)	α^c
PEP 1000	Extracted	262 (552)	2.10	135.9	144.4	54
	Residual	—	—	132.9	51.4[b]	19
PEP 700	Extracted	155 (416)	2.68	134.4	155.3	58
	Residual	—	—	133.0	56.5 [b]	21
PEP 500	Extracted	178 (446)	2.51	137.9	183.5	68
	Residual	—	—	130.0	58.4 [b]	22
PEP 300	Extracted	284 (617)	2.17	133.6	164.3	61
	Residual	—	—	130.6	40.7 [b]	15

[a] Catalytic system: GTR (toluene suspension) then MAO (60′ at 60°C) + Cp_2ZrCl_2 (150′ at 80°C).
[b] Normalized with respect to the PE content (in grams) in the composite. Note that for extracted PEs the PE content is 100%.
[c] α = % crystallinity = $\Delta H_{m,sample}$/(269.9 J/g). The value ΔH_m = 269.9 J/g is referred to 100% crystalline PE.

absence of GTR) shows a $<M_w>$ of 514 kDa (MWD = 1.97). The MWDs indexes were slightly higher than in GTR-free polymerizations (where these values seldom exceed 2); moreover, the observed presence of enlarged peaks, sometimes having shoulders, could account for bimodal or pluri-modal MW distributions. Again, this experimental evidence suggests the presence of different active sites producing various macromolecules, both of which partly (or wholly) extractable with boiling xylene.

The crystallinity of the residual PE is strictly lower than that of extracted fractions, as well as the T_m (Table I). This evidence is in agreement with the hypothesis of two different active sites: one of them, operating *far from the support* produces PE macromolecules having high T_m and α (these macromolecules are extractable in xylene); the other ones produce PE having low T_m and α (these macromolecules are only partially extractable in xylene).

In order to better investigate the nature of the catalyst sites, a filtration of the filler treated with MAO (Al/Zr feed ratio: 1000) was performed in order to eliminate the unanchored co-catalyst. The system was later used as supported catalyst system for ethylene polymerization.

The PE content of the obtained composite (named *Al-filtered*) was 91.1 wt %, similar to that of PEP 1000 (91.8 wt %); TGA analysis (90.1 wt %) confirmed the data. Also the catalyst productivity was similar to that of PEP 1000: (171 ± 10) against (177 ± 10) $kg_{PE}/(n_{Zr}$ bar hour), respectively.

DSC analysis showed a T_m of 136.4°C and a crystallinity degree of 57; the α is slightly lower than in PEP 1000. The resulting grafting efficiency after xylene extraction was higher with respect to the other composites (17.5% against ~9%–12%), and the residual showed a high PE content (61.6 wt %).

SEC analysis of the extracted fraction showed a very high value of molecular weight: $<M_n>$ = 487 kDa ($<M_w>$ = 1103 kDa) with MWD = 2.27. Probably the filtration reduced the total amount of active sites, or reduced the occurring of transfer reactions due to the absence of unanchored MAO, thus producing PE chains with higher MW. The composite was also characterized by a higher percentage of unextractable PE; this evidence confirms a reduction of active sites working in solution with respect to the ones located near to the GTR surface or penetrated in the bulk of the filler particles, which are probably the responsible of the unextractable polymer production.

Effect of the Reaction Time

By keeping constant the Al/Zr ratio to 500, that resembled a good compromise between the amount of MAO used and catalyst productivity, several polymerization experiments were carried out by quenching the runs at different times; the catalyst activities over time are reported in Figure 7.

An initial increment is followed, over time, by a decrement. This is a common result, observed also in homogeneous metallocenic polymerizations, and it is often attributed to the deactivation of the catalytic centers along with the decreased monomer diffusion capability toward the active sites through the PE growing chains.[47] On the other side, the initial increment is due to the process of monomer diffusion in the solvent toward the active centers; in a study concerning the ethylene polymerization onto zeolites with the same catalyst system (Cp_2ZrCl_2/MAO) adopted in the present study, a very slight increment of the activity over time was observed up to

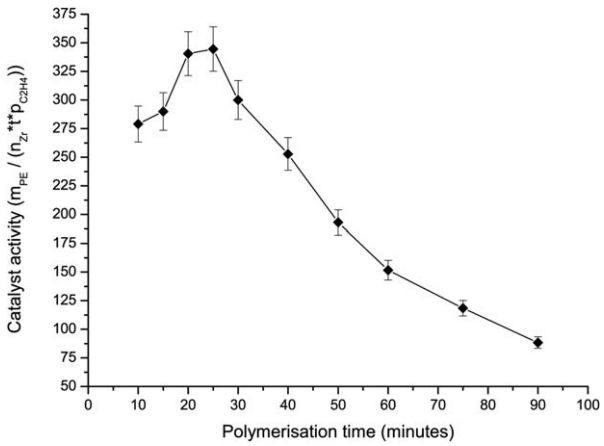

Figure 7. Catalyst productivity versus polymerization time.

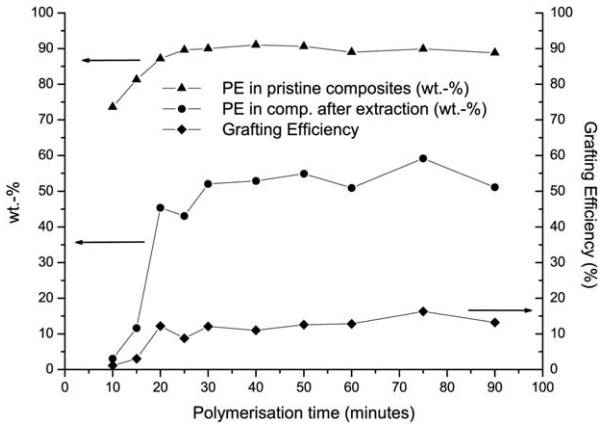

Figure 8. PE content in composites before and after the extraction (left *y*-axis), and grafting efficiency (right *y*-axis) versus polymerization time.

polymerization times of nearly 60 min. This increment is probably due to the peculiar morphology of the support that slowed down monomer diffusion, and emphasized the activity increment over time (average productivity). The main factor influencing the induction time is the monomer solubility in the reaction medium and its kinetics; a key role is then played by the monomer pressure over the solution, the reaction temperature, and the nature of the support.

In Figure 8 the PE content in the pristine composites, in the residual composites after 16-hours xylene extraction and the grafting efficiencies are reported.

The amount of PE increases over time up to a constant value, as well as the amount of PE in the extracted compounds and the grafting efficiency; in other words, there are no meaningful variations in terms of hybrid constitution/composition. This is a direct consequence of the catalytic productivity decrement at high polymerization times. At low polymerization times, instead, the small values of grafting efficiency suggest that the formed PE chains are mostly extractable, thus evidencing that their formation is not generating/taking part to the sIPN structure.

The extracted fractions were characterized by IR, ^{13}C-NMR, DSC, and SEC. While IR and NMR spectroscopies did not highlight variations in the PE primary structure (branching degree: at most one tertiary carbon every 12,000 atoms for every sample), SEC showed that most of the molecular weight distributions were bimodal, except those of samples synthesized within short polymerization times. A summary of SEC and DSC data regarding extracted fractions and DSC data of some residual fractions are reported in Table V; thermograms of residual samples of PEP 25′/30′/40′ were the only ones in which a T_m was evident.

In any case, no particular trends regarding the molecular weights were detectable except a slight overall growth over polymerization time ($<M_n>$ varied from 120 to 180 kDa); all the molecular weight distributions showed a bimodal trend, even if by increasing the polymerization time the two populations gradually merged in a larger curve, as assessed by polydispersity data. Even T_ms and crystallinity values of the extracted parts showed only minor variations, and in a small range (between 132°C and 137°C for T_m, between 55% and 65% for the crystallinity values). Instead, the residual PE fractions after xylene

Table V. SEC Measurements and Thermal Properties (by DSC) of the PEP Produced by Changing the Reaction Time Samples After Xylene Extraction

Sample		$<M_n>$ ($<M_w>$) kDa	MWD	DSC data		
				T_m (°C)	ΔH_m (J/g)	α[d]
PEP 10′	Extracted	124 (408)	3.30	133.6	148.5	55.0
PEP 15′	Extracted	304 (758)	2.49	135.7	155.0	57.4
PEP 20′	Extracted	119 (435)	3.65	133.9	164.1	60.8
PEP 25′ [a]	Extracted	57/629[b]	1.26	137.1	169.1	62.7
		(115/791)	2.00			
	Residual	—	—	~122.2	10.7 [c]	9.2
PEP 30′ [a]	Extracted	46/560[b]	1.29 2.10	132.1	171.5	63.5
		(96/724)				
	Residual	—	—	~126.7	14.2 [c]	10.1
PEP 40′ [a]	Extracted	48/617[b]	1.22 2.44	135.9	164.0	60.8
		(112/758)				
	Residual	—	—	~123.4	20.2 [c]	14.1
PEP 50′	Extracted	121 (586)	4.83	134.7	173.2	64.2
PEP 60′	Extracted	128 (520)	4.07	132.9	175.3	64.9
PEP 75′	Extracted	152 (704)	4.61	132.3	150.9	55.9
PEP 90′	Extracted	178 (724)	4.06	130.1	137.8	51.1

[a] T_m in extraction residues was evident only for samples PEP 25′/30′/40′.
[b] Bimodal molecular weight distribution.
[c] Normalized with respect to the PE content (in grams) in the composite. Note that for extracted PEs the PE content is 100%.
[d] α = % crystallinity = $\Delta H_{m,sample}$/(269.9 J/g). The value ΔH_m = 269.9 J/g is referred to 100% crystalline PE.

Table VI. Tensile Properties of the Samples

Sample	GTR (wt %)	Strength at yield (MPa)	Elongation at yield (%)	Strength at break (MPa)	Elongation at break (%)	Young's modulus (MPa)
PEP 2	8.8	20.2	5.2	25.8	201.8	1014
SimpleMix [a]	8.8	22.2	4.2	22.2	6.8	1396
ComplexMix [b]	8.8	19.1	4.2	20.4	9.6	1031
PE 2	0	23.0	4.6	37.0	486.9	1154
HDPE	0	32.1	4.3	36.8	31.7	1826

[a] Obtained by simply mixing HDPE and GTR.
[b] Obtained by mixing HDPE with PEP 10′.

extraction of experiments PEP 25′/30′/45′ show values of α not >15%, and T_ms are in the range 122°C–127°C.

This evidence confirms, once again, that two macromolecular populations are synthesized, one from catalyst system present in the solvent and not supported onto the GTR (like in the case of *in-situ* polymerization approach) and one inside the GTR; the first macromolecules are produced in solution (this explains the small grafting efficiency at low polymerization times). With higher reaction times, both typical HDPE macromolecules are formed in solution and macromolecules having low crystallinity inside the GTR; the first ones are extractable in xylene, the second ones are only partly extractable (this explains why extracted fractions have bimodal molecular weight distribution and why residual fractions are composed of GTR and scarcely crystalline PE chains).

Preliminary Tensile Properties of PE/GTR Composites

In order to investigate the mechanical properties of PE/GTR composites produced with different methodologies, some tensile tests were performed according to the ASTM D 638 procedure.[48] Strength (σ_y) and elongation (ε_y) at yield, strength (σ_B) and elongation (ε_B) at break, and Young's modulus (E') were determined. Three different PE/GTR composites containing the same final amount of GTR were examined: (i) a composite obtained by *in-situ* catalytic polymerization of ethylene in the presence of GTR following PFT procedure: PEP 2; (ii) a composite obtained by melt blending a commercial HDPE with GTR: SimpleMix; and (iii) a composite obtained by melt blending a commercial HDPE with a composite obtained by PFT: ComplexMix.

The mechanical characteristics for all the samples were also compared with those of sample PE 2 resembling the matrix of composite PEP 2 and of HDPE used as matrix of SimpleMix and ComplexMix composites (Table VI).

It is necessary to underline that the mechanical characteristics of the two matrices (PE 2 and HDPE) are quite different in terms of elongation at break and Young's modulus. In particular, the latter was more rigid and with a lower elongation at break; this can be attributed to the different type of macromolecular chains and crystalline domains. The macromolecular chains of the commercial sample were shorter compared with those of the sample obtained by PFT ($<M_n>$ = 70 kDa for HDPE, $<M_n>$ = 170 kDa for PE 2) and the crystallinity degree was higher (α_{HDPE} = 77.1%, $\alpha_{PE\ 2}$ = 57.6%).

By comparing the composite PEP 2 with its possible matrix, lower Young's modulus was observed (ca., −12%), suggesting the effectiveness of the PFT in producing composites with reduced stiffness. The same trend can be envisaged by comparing the composites prepared by melt mixing with their matrix, HDPE, but better performances were showed for the sample ComplexMix prepared by dispersing a PE/GTR composite, suggesting the toughening of the matrix presumably owing to enhanced interfacial adhesion/interactions when the GTR particles are covered by PE shells or embedded by PE macromolecules growth inside the particles. The comparison in tensile behavior of all the composites PEP 2, SimpleMix, and ComplexMix (even if prepared on the basis of different matrices) evidenced that PEP 2 had lower Young's modulus and strength at yield and higher elongation at yield and at break, confirming the PFT as a viable methodology to produce toughened composites starting from GTR particles.

FINAL REMARKS

Novel hybrid composites with HDPE matrix and powdered rubber coming from scrap tyres (GTR) were prepared through catalytic polymerization of ethylene by employing different methodologies: the *in-situ* polymerization and the *PFT*. The first method provides for the catalytic polymerization of ethylene in solution in the presence of GTR swollen particles, while the PFT approach foresees the use of GTR-supported catalyst. This last was prepared and carefully characterized, polymerization conditions being optimized in terms of catalyst productivity and grafting efficiency by changing the support (GTR) treatment conditions, the catalyst/co-catalyst ratio and the time of reaction. The PFT technique (instead of *in-situ* polymerization) clearly evidenced the capability to generate macromolecules growing inside the particles thus producing a sIPN structure between the HDPE macromolecules and the rubber network. The establishment of this architecture is responsible for a breaking-up effect of the rubber particles, which promotes the interfacial interactions and enhances the final mechanical features of the hybrid composites. In particular, a clear improvement of the stress–strain behavior of the hybrid materials or composites based onto samples produced by PFT approach with respect those prepared by conventional melt mixing of HDPE and GTR particles was observed and associated to the sIPN morphology due to the described polymerization procedure.

The results here collected clearly prove that this approach provides samples with morphologies that appear promising for the thermo-mechanical behavior of these hybrid materials, as it was partially proved by preliminary tensile tests. New insights

concerning the mechanical and the rheological properties are currently in progress.

ACKNOWLEDGMENTS

Pirelli Labs S.p.A is acknowledged for financial support. Dr Piero Schiavuta is acknowledged for his kind help in the particles size distribution analysis and Dr. Yi Thomann for her support in AFM analysis.

REFERENCES

1. Sienkiewicz, M.; Kucinska-Lipka, J.; Janik, H.; Balas, A. *Waste Manage.* **2012**, *32*, 1742.
2. Rizzi, F.; Bartolozzi, I.; Borghini, A.; Frey, M. *Bus. Strat. Environ.* **2013**, *22*, 561.
3. Adhikari, B.; De, D.; Maiti, S. *Prog. Polym. Sci.* **2000**, *25*, 909.
4. Rajeev, R. S.; De S. K. *Rubb. Chem. Technol.* **2004**, *77*, 569.
5. Fang, Y.; Zhan, M.; Wang, Y. *Mater. Des.* **2001**, *22*, 123.
6. Jacob, C.; De, S. K. In Rubber Recycling; De, S. K.; Khait, K.; Isayev, A., Eds.; CRC Press, Boca Raton, **2005**; Chapter *6*.
7. Khait K. In Rubber Recycling; De, S.K.; Khait, K.; Isayev, A., Eds.; CRC Press, Boca Raton, **2005**; Chapter *4*.
8. Mangaraj D. *Rubb. Chem. Technol.* **2005**, *78*, 536.
9. Rajeev, R. S.; De, S. K. *Rubb. Chem. Technol.* **2004**, *77*, 569.
10. Srinivasan, A.; Shanmugharaj, A. M.; Bhowmick, A. K. In Current Topics in Elastomers Research; Bhowmick, A. K., Eds.; CRC Press, Boca Raton, **2008**, Chapter *38*, p 1043.
11. Prun, E.; Kuznetsova, O.; Karger-Kocsis, J.; Solomatin, D. *J. Reinf. Plast. Compos.* **2012**, *31*, 1758.
12. Kakroodi, A. R.; Rodrigue, D. *Polym. Degrad. Stabil.* **2013**, *98*, 2184.
13. Mészáros, L.; Bárány, T.; Czvikovszky, T. *Radiat. Phys. Chem.* **2012**, *81*, 1357.
14. Cañavate, J.; Casas, P.; Colom, X.; Nogués, F. *J. Compos. Mater.* **2011**, *45*, 1189.
15. Mészáros, L.; Fejős, M.; Bárány, T. *J. Appl. Polym. Sci.* **2012**, *125*, 512.
16. Colom, X.; Cañavate, J.; Carrillo, F.; Lis M. J. *J. Compos. Mater.* doi: 10.1177/0021998313482154, to appear.
17. Karger-Kocsis, J.; Mészáros, L.; Bárány, T. *J. Mater. Sci.* **2013**, *48*, 1.
18. Fuhrmann, I.; Karger-Kocsis, J. *J. Appl. Polym. Sci.* **2003**, *89*, 1622.
19. Zhang, X.; Zhu, X.; Liang, M.; Lu, C. *J. Appl. Polym. Sci.* **2009**, *114*, 1118.
20. Kocevski, S.; Yagneswaran, S.; Xiao, F.; Punith, V. S.; Smith Jr. D. W.; Amirkhanian, S. *Constr. Build. Mater.* **2012**, *34*, 83.
21. Wang, L.; Lang, F.; Li, S.; Du, F.; Wang, Z. *J. Thermopl. Comp. Mater.* doi: 10.1177/0892705712473628, to appear.
22. Wang, Z.; Zhang, Y.; Du, F.; Wang, X. *Mater. Chem. Phys.* **2012**, *136*, 1124.
23. Johnson, L. D. (Synesis Corporation). US Patent 5,157,082, October 20, **1992**.
24. Coiai, S.; Ciardelli, F.; Passaglia E.; Sulcis, R.; Resmini,E.; Tirelli, D.; Peruzzzotti, F. US Patent 0,132,642 A1 June 18, **2008**.
25. Dubois, P.; Alexandre, M.; Hindryckx, F.; Jerome, R. *J. Macromol. Sci., Rev. Macromol. Chem. Phys.* **1998**, *C38*, 511.
26. Wang, L.; Feng, L.-X.; Xie, T. *Polym. Int.* **2000**, *49*, 184.
27. Alexandre, M.; Martin, E.; Dubois, P.; Garcia-Marti, M.; Jerome, R. *Macromol. Rapid Commun.* **2000**, *21*, 931.
28. Alexandre, M.; Pluta, M.; Dubois, P.; Jerome, R. *Macromol. Chem. Phys.* **2001**, *202*, 2239.
29. Stuürzel, M.; Kempe,F.; Thomann, Y.; Mark, S.; Enders, M.; Muülhaupt, R. *Macromolecules* **2012**, *45*, 6878.
30. Francq, R.; Persenaire, O.; Alexandre, M.; Degèe, P.; Dubois, P. e-polymers 2002, P_044.
31. Bonduel, D.; Mainil, M.; Alexandre, M.; Monteverde, F.; Dubois, P. *Chem. Commun.* **2005**, *6*, 781.
32. Kaminsky, W.; Funck, A.; Klinke, C. *Top. Catal.* **2008**, *48*, 84.
33. Alexandre, M.; Dubois, P.; Sun, T.; Garces, J. M.; Jerome, R. *Polymer* **2002**, *43*, 2123.
34. Leone, G.; Bertini, F.; Canetti, M.; Boggioni, L.; Stagnaro, P.; Tritto, I. *J. Polym. Sci.Part A: Polym. Chem.* **2008**, *46*, 5390.
35. Heinemann, J.; Reichert, P.; Thomann, R.; Mulhaupt, R. *Macromol. Rapid Commun.* **1999**, *20*, 423.
36. Carrero, A.; van Grieken, R.; Suarez, I.; Paredes, V. *J. Appl. Polym. Sci.* **2012**, *126*, 987.
37. Weiss, K.; Wirth-Pfeifer, C.; Hofmann, M.; Botzenhardt, S.; Lang, H.; Bruning, K.; Meichel, E. *J. Mol. Catal. Part A: Chem.* **2002**, *182/183*, 143.
38. Halbach, T. S.; Mülhaupt, R. *Polymer* **2008**, *49*, 867.
39. Cao, X.; Feng, L. *Eur. Polym. J.* **2000**, *36*, 2243.
40. Coiai, S.; Passaglia, E.; Ciardelli, F.; Tirelli, D.; Peruzzotti, F.; Resmini, E. *Macromol. Symp.* **2006**, *234*, 193.
41. Pluta, M.; Alexandre, M.; Blacher, S.; Dubois, P.; Jerome, R. *Polymer* **2001**, *42*, 9293.
42. Bertini, F.; Canetti, M.; Leone, G.; Tritto, I. *J. Anal. Appl. Pyrolysis* **2009**, *86*, 74.
43. Ravasio, A.; Boggioni, L.; Tritto, I.; D'Arrigo, C.; Perico, A.; Hitzbleck, J.; Okuda, J. *J. Polym. Sci. Part A: Polym. Chem.* **2009**, *47*, 5709.
44. Chien, J. C. W.; He, D. *J. Polym. Sci. Part A: Polym. Chem.* **1991**, *29*, 1603.
45. Panchenko, V. N.; Zakharov, V. A.; Danilova, I. G.; Paukshtis, E. A.; Zakharov, I. I.; Goncharov, V. G.; Suknev, A. P. *J. Mol. Catal.Part A: Chem.* **2001**, *174*, 107.
46. Zimnoch dos Santos, J. H.; Krug, C.; Barbosa da Rosa, M.; Stedile, F. C.; Dupont, J.; Forte, M. d. C. *J. Mol. Catal.Part A: Chem.* **1999**, *139*, 199.
47. McKenna, T. F.; Soares, J. B. P. *Chem. Eng. Sci.* **2001**, *56*, 3931.
48. ASTM D 638, Standard Test Method for Tensile Properties of Plastics, **1995**.